Meiotic interference among MLH1 foci requires neither an intact axial element structure nor full synapsis

Esther de Boer[1], Axel J. J. Dietrich[2], Christer Höög[3], Piet Stam[4] and Christa Heyting[1,*]

[1]Wageningen University, Molecular Genetics group, Arboretumlaan 4, 6703 BD Wageningen, The Netherlands
[2]Institute of Human Genetics, University of Amsterdam, AMC, Meibergdreef 9, 1105 AZ Amsterdam, The Netherlands
[3]Department of Cell and Molecular Biology, Karolinska Institute, SE-171 77 Stockholm, Sweden
[4]Wageningen University, Laboratory of Plant Breeding, Droevendaalsesteeg 1, 6708 PB Wageningen, The Netherlands
*Author for correspondence (e-mail: Christa.Heyting@wur.nl)

Accepted 4 January 2007
Journal of Cell Science 120, 731-736 Published by The Company of Biologists 2007
doi:10.1242/jcs.003186

Summary

During meiosis, homologous chromosomes (homologs) perform reciprocal exchanges (crossovers) at a high frequency. Crossovers display interference, i.e. their spacing is more even than would be expected if they were placed randomly along the chromosomes. Concomitantly with crossover formation, synaptonemal complexes (SCs) appear between homologs: each chromosome forms an axial structure, the axial element (AE); the AEs of homologs align, and numerous transverse filaments connect the AEs to form an SC. Both the AE and the SC have been implicated in the imposition of interference. We investigated whether intact AEs or SCs are required for crossover interference in the mouse, using a mutant lacking AE protein SYCP3, which displays structurally abnormal AEs and incomplete synapsis. We estimated the level of interference from the spacing of immunofluorescent MLH1 foci, which mark almost all crossover sites in the mouse, along the SCs. The levels of interference among MLH1 foci in wild-type and *Sycp3*$^{-/-}$ mice were comparable, implying that neither an intact AE structure nor full synapsis is required for wild-type levels of interference.

Supplementary material available online at
http://jcs.biologists.org/cgi/content/full/120/5/731/DC1

Key words: Meiosis, Synapsis, Axial elements, Interference, MLH1, Mouse

Introduction

During the prophase of the first meiotic division, homologous chromosomes (homologs) form stable pairs (bivalents), and non-sister chromatids of homologs exchange corresponding parts. Concomitantly, a zipper-like structure, the synaptonemal complex (SC), is formed between the homologs (Page and Hawley, 2004): the two sister chromatids of each chromosome form a common axis, the axial element (AE), and the AEs of homologs are connected along their length by transverse filaments, a process called synapsis, to form an SC. Along AEs and SCs, protein complexes occur that are involved in homologous chromosome pairing and crossover formation, and can be visualized as foci by immunofluorescence labeling (Ashley and Plug, 1998). One component of such protein complexes is the *Escherichia coli* MutL-homologous protein MLH1, which participates in a late step in crossover formation (Baker et al., 1996; Hunter and Borts, 1997). In the mouse, the number and spatial distribution of MLH1 foci along bivalents closely correspond with those of crossovers (Broman et al., 2002; Froenicke et al., 2002).

Crossovers are more evenly spaced along bivalents than is to be expected if they were placed randomly, a phenomenon named (positive) crossover interference. In early interference models, important roles were ascribed to SCs and/or synapsis (reviewed by Egel, 1995), but evidence against this is accumulating (reviewed by de Boer and Heyting, 2006). AEs, on the other hand, are still considered potentially important for crossover interference (Hillers, 2004; Kleckner and Zickler, 2003; Nabeshima et al., 2004).

We analyzed whether full synapsis and/or structurally intact AEs are required for crossover interference in the mouse, by studying cytological interference among MLH1 foci in *Sycp3*$^{-/-}$ mice, which display structurally abnormal AEs and incomplete synapsis. The level of interference among MLH1 foci was the same in these mice as in the wild type, and we conclude therefore that crossover interference requires neither intact AEs nor full synapsis.

Results and Discussion

During meiotic prophase of *Sycp3*$^{-/-}$ mice, the two sister chromatids of each chromosome still form a common axial structure, which contains cohesins, but lacks AE proteins SYCP3 and SYCP2 (Pelttari et al., 2001). This structure, further denoted as 'cohesin axis', appears stretched and fragmented when visualized by labeling of cohesins in spread *Sycp3*$^{-/-}$ spermatocytes or oocytes (Fig. 1) (Pelttari et al., 2001). *Sycp3*$^{-/-}$ cohesin axes synapse incompletely and discontinuously (Fig. 1A,B) (Pelttari et al., 2001). Whereas *Sycp3*$^{-/-}$ spermatocytes enter apoptosis presumably before MLH1 foci appear (Yuan et al., 2000), *Sycp3*$^{-/-}$ oocytes assemble MLH1foci, and in some cases form chiasmata and complete meiosis (Yuan et al., 2002). The formation of MLH1 foci in *Sycp3*$^{-/-}$ oocytes provided a unique opportunity to investigate at the cytological level the role of AEs and synapsis

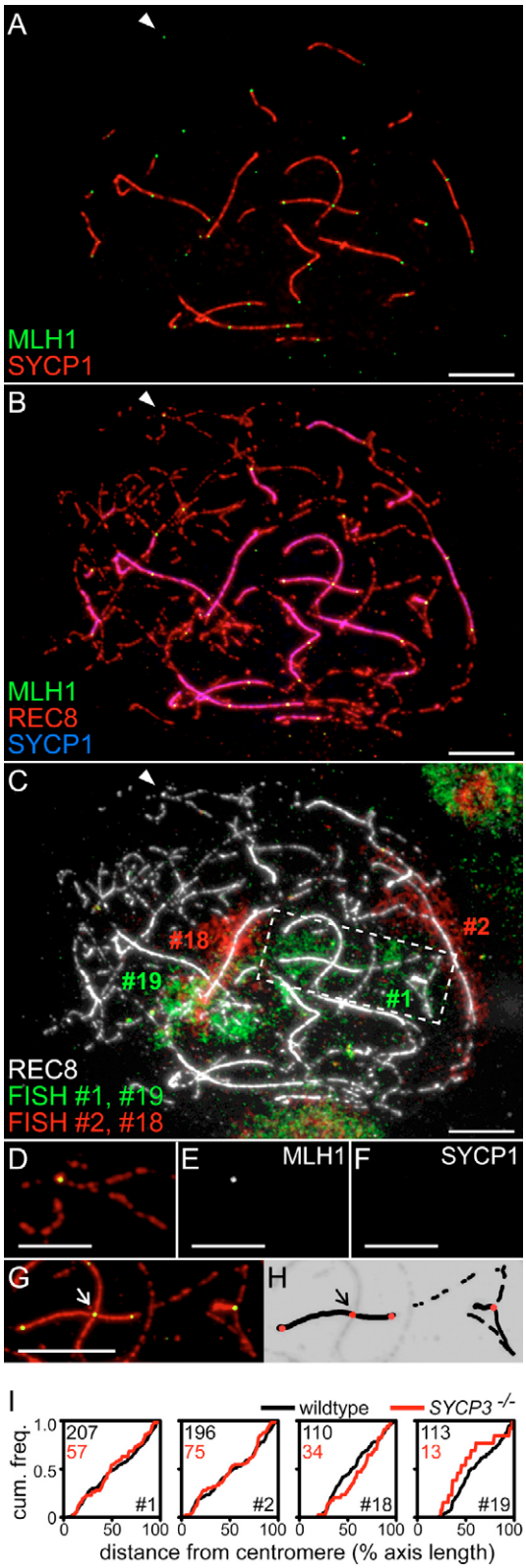

Fig. 1. Analysis of MLH1 foci along bivalents. (A) Spread *Sycp3*$^{-/-}$ oocyte labeled for SYCP1 and MLH1. (B) Merged image of the signals for MLH1, SYCP1 and meiotic cohesin REC8 on the same oocyte as in A. SYCP1 was always found on converged cohesin axes; regions of synapsis are visible as pink stretches of converged cohesin axes in this panel. (C) Merged image of the REC8 and the FISH signals on the same oocyte as in A. The FISH probes label chromosomes 1 (green), 2 (red), 18 (red) and 19 (green). The arrowhead in panels A-C indicates an MLH1 focus on two converged cohesin axes in the absence of detectable SYCP1. (D-F) Cut outs of panels A-C, showing part of the bivalent carrying the MLH1 focus indicated by the arrowhead. (D) Merged image of the MLH1, SYCP1 and REC8 signals; (E) the MLH1 signal; (F) the SYCP1 signal. (G,H) Cut out of panel C, showing the merged MLH1 and REC8 signals of chromosome 1 (G), and a reconstruction of chromosome 1, with REC8 represented in black and MLH1 in red (H). The arrow indicates an MLH1 focus at the crossing of cohesin axes of different bivalents; bivalent segments carrying such foci are excluded from the analysis. (I) Distributions of MLH1 foci along bivalents. Shown are the cumulative frequencies of MLH1 foci as a function of the distance to the centromeric end of the SC (wild type; black line) or cohesin axis (*Sycp3*$^{-/-}$; red line). The distances are expressed as a percentage of the length of the SC (cohesin axis) on which the focus was. The numbers of foci on which the curves are based are shown in the upper left corners, and the chromosome numbers in the lower right corners of the graphs. Bars, 10 μm.

in interference, even in cells that cannot form chiasmata and complete meiosis.

We studied interference among MLH1 foci in oocytes at day 18 post coitus, when the proportion of MLH1-positive nuclei reached its maximum, both in *Sycp3*$^{-/-}$ and wild-type mice (not shown). We focused on two long (1 and 2) and two short (18 and 19) chromosomes, which we identified by FISH (Fig. 1C). Because we inferred the strength of interference among MLH1 foci from the frequency distribution of interfocus distances (see below), it was essential that we could unambiguously recognize and locate every individual MLH1 focus on the cohesin axis. Therefore, we only analyzed bivalents of which: (1) both ends could be recognized; (2) at least one cohesin axis could be fully traced; and (3) all MLH1 foci could be clearly distinguished from background signals. Only 15% of the FISH-labeled bivalents in MLH1-positive oocytes fulfilled these criteria (see Fig. S1 in supplementary material). When measuring distances along cohesin axes, we excluded the gaps between the signals for meiotic cohesin REC8, for reasons explained in supplementary material Table S1 and Fig. S1Q,R.

MLH1 foci on *Sycp3*$^{-/-}$ bivalents

In *Sycp3*$^{-/-}$ oocytes, MLH1 foci were located in regions of synapsis (identified by the presence of TF-protein SYCP1; Fig. 1A) or at sites where cohesin axes converged without detectable SYCP1 (Fig. 1A,B,D-F) (cf. Higgins et al., 2005), whereas they were lacking from the paracentromeric region on all four analyzed chromosomes, in both *Sycp3*$^{-/-}$ and wild-type mice (cf. de Boer et al., 2006; Froenicke et al., 2002). In the wild type, MLH1 foci were distributed rather uniformly along the remainder of the chromosomes, and this pattern was maintained on *Sycp3*$^{-/-}$ chromosomes 1 and 2. For *Sycp3*$^{-/-}$ chromosomes 18 and 19, the numbers of analyzed MLH1 foci were too small to decide whether they were distributed similarly along the bivalents as in the wild type (Fig. 1I).

The average number of MLH1 foci per oocyte nucleus was lower in *Sycp3*$^{-/-}$ than in wild-type mice (Table 1), which fits with the decreased number of chiasmata in *Sycp3*$^{-/-}$ oocytes (Yuan et al., 2002). Nevertheless, three of the four analyzed chromosomes had similar numbers of MLH1 foci in *Sycp3*$^{-/-}$ and wild-type oocytes (Table 1); only on *Sycp3*$^{-/-}$ chromosome

Table 1. Density of MLH1 foci in *Sycp3*$^{-/-}$ and wild-type oocytes

Genotype	MLH1 foci per nucleus*	MLH1 foci per bivalent†			
		Chromosome 1	Chromosome 2	Chromosome 18	Chromosome 19
Wild type	27.6±3.5 (64)	1.85±0.56 (112)	1.78±0.51 (110)	1.05±0.32 (105)	1.00±0.23 (113)
Sycp3$^{-/-}$	21.4±3.9‡ (64)	1.82±0.72 (44)	1.83±0.60 (47)	1.04±0.35 (49)	0.79±0.50‡ (28)

*Mean ± s.d. (number of nuclei analyzed).
†Mean ± s.d. (number of bivalents analyzed).
‡Significantly different from the wild type (P<0.01; unpaired Student's t-test).

Table 2. Interference among MLH1 foci in wild-type and *Sycp3*$^{-/-}$ oocytes

Genotype	Chromosome*	Number of intervals	Average interfocus distance (s.d.)		$\hat{\nu}$ (s.e.)†	P‡	Corr. ν§
			μm	% SC			
Wild type	1	95	7.2 (2.8)	51.4 (16.3)	8.9 (1.3)	0.3	7.5
	2	88	7.1 (2.3)	52.7 (14.9)	11.7 (1.7)	0.3	10.1
Sycp3$^{-/-}$	1 (total)	31	12.4 (3.2)	42.6 (12.7)	11.5 (2.9)	0.2	10.0
	1 syn.	15	11.5 (3.2)	41.9 (14.8)	9.5 (3.4)	0.5	
	1 unsyn.	16	13.3 (3.1)	43.2 (10.8)	14.5 (5.1)	0.4	
	2 (total)	36	13.9 (5.0)	48.2 (17.0)	8.5 (2.0)	0.05	7.3
	2 syn.	18	12.1 (3.4)	41.8 (12.9)	12.1 (4.0)	0.2	
	2 unsyn.	18	15.6 (5.7)	54.5 (18.6)	8.4 (2.7)	0.03	

*For *Sycp3*$^{-/-}$, total relates to all inter-MLH1 intervals; syn. to fully synapsed inter-MLH1 intervals; and unsyn. to fully or partially unsynapsed inter-MLH1 intervals on bivalents of chromosome 1 and 2.
†Maximum likelihood estimate of the interference parameter ν in the gamma model (with estimated standard error s.e.).
‡Estimated P value; P is the probability of finding an as-bad or worse fit of the observed interfocus distances to the gamma distribution because of sampling error.
§$\hat{\nu}$ corrected (corr.) for the limited range of observable interfocus distances; the correction results in slightly lower estimates of ν (cf. de Boer et al., 2006).

19 was the number of MLH1 foci reduced. Accordingly, Yuan et al. (Yuan et al., 2002) reported a differential effect of the *SYCP3* disruption on recombination on different chromosomes. Among the chromosomes analyzed by these authors chromosome 12 displayed reduced recombination in a *Sycp3*$^{-/-}$ background. Both chromosome 19 and chromosome 12 carry a nucleolus-organizing region (Dev et al., 1977). Possibly these chromosomes pair later than average, and in a *Sycp3*$^{-/-}$ background part of them might pair too late to form MLH1 foci.

Wild-type levels of interference among MLH1 foci in *Sycp3*$^{-/-}$ oocytes

As is explained in detail elsewhere (Broman et al., 2002; de Boer et al., 2006; McPeek and Speed, 1995; Stam, 1979), the strength of interference among foci can be estimated by fitting the frequency distribution of interfocus distances to the gamma distribution. This yields an estimate of the so-called interference parameter of the gamma model, here denoted by ν, which is a measure of the strength of interference: if the best fit is obtained for ν=1, there is no interference, and the higher ν is above 1, the stronger (positive) interference is.

Since chromosomes 18 and 19 rarely have more than one MLH1 focus (Table 1), we could only estimate the strength of interference from the interfocus distances on chromosomes 1 and 2. As judged by the P values in Table 2, the interfocus distances on these chromosomes fitted reasonably to the gamma distribution. In wild-type oocytes, the estimates of ν ($\hat{\nu}$ values in Table 2) for chromosomes 1 and 2 were high, 8.9 and 11.7 respectively, indicating strong interference among MLH1 foci on these chromosomes. For *Sycp3*$^{-/-}$ oocytes, we obtained similarly high $\hat{\nu}$ values (Table 2), indicating a similar high interference level among MLH1 foci in *Sycp3*$^{-/-}$ oocytes as in the wild type. Intact AEs are thus not required for wild-type interference levels.

In *Sycp3*$^{-/-}$ oocytes, the cohesin axes between two MLH1 foci were often not (fully) synapsed (Fig. 1A-H). To analyze whether synapsis had any influence on interference, we compared interference among MLH1 foci that were separated by fully synapsed cohesin axes with interference among foci that were separated by stretches of unsynapsed or incompletely synapsed cohesin axes. For both situations, we obtained similar high $\hat{\nu}$ values (Table 2), indicating that full synapsis is not required for wild-type interference levels among MLH1 foci.

Estimating interference levels from the distributions of the numbers of foci per bivalent

The ν estimates (Table 2) are based on the observed interfocus distances, and thus only on bivalents with two or more foci. Interference levels can also be estimated from the distributions of the numbers of foci per bivalent. Although this approach is generally less valuable than the approach based on interfocus distances (see Broman and Weber, 2000), it has the advantage that bivalents with fewer than two foci can be included in the analysis. Therefore, we determined for each of the four analyzed chromosomes, in *Sycp3*$^{-/-}$ and wild-type oocytes, the proportions of bivalents with 0, 1, 2, 3 and 4 foci. For chromosome 19, we found a significant difference between *Sycp3*$^{-/-}$ and the wild type, as was to be expected, because chromosome 19 bivalents had on average fewer MLH1 foci in *Sycp3*$^{-/-}$ than in wild-type oocytes (Table 1). For chromosomes 1, 2 and 18, there was no significant difference between *Sycp3*$^{-/-}$ and wild-type oocytes (Table 3).

Using computer simulation, and assuming that the MLH1

Table 3. Distributions of the numbers of MLH1 foci per bivalent

Chromosome	Genotype (number of bivalents)	Observed or expected*	Percentage of bivalents with: 0 foci	1 focus	2 foci	3 foci	4 foci	Observed vs expected $P^{\dagger}$	Obs. wt vs obs. –/– $P^{\ddagger}$
1	Wild type (112)	Observed	0.0	24.1	67.0	8.9	0.0	0.31	0.15
		Exp. (ν=8)§	0.4	26.9	60.3	12.2	0.2		
	Sycp3$^{-/-}$ (44)	Observed	4.6	22.7	59.1	13.6	0.0	0.98	
		Exp. (ν=10)§	0.3	27.2	63.0	9.5	0.1		
2	Wild type (110)	Observed	1.8	20.9	74.6	2.7	0.0	0.01	0.40
		Exp. (ν=10)§	0.3	29.8	61.6	8.3	0.0		
	Sycp3$^{-/-}$ (47)	Observed	2.1	21.3	68.1	8.5	0.0	0.36	
		Exp. (ν=7)§	0.8	28.5	58.0	12.5	0.3		
18	Wild type (105)	Observed	2.9	89.5	7.6	0.0	0.0		0.91
		Exp. (ν=1)¶	35.0	37.0	19.4	6.8	2.8	4.7×10^{-27}	
		Exp. (ν=17)**	7.2	80.5	12.2	0.0	0.0	0.06	
	Sycp3$^{-/-}$ (49)	Observed	4.1	87.8	8.2	0.0	0.0		
		Exp. (ν=1)¶	35.5	36.9	19.3	6.6	1.7	1.4×10^{-12}	
		Exp. (ν=8)**	11.6	73.0	15.3	0.1	0.0	0.06	
19	Wild type (113)	Observed	2.7	94.7	2.7	0.0	0.0		0.0004
		Exp. (ν=1)¶	37.0	36.9	18.4	6.1	1.5	1.3×10^{-12}	
		Exp. (ν=33)**	6.1	87.8	6.1	0.0	0.0	0.08	
	Sycp3$^{-/-}$ (28)	Observed	25.0	71.4	3.6	0.0	0.0		
		Exp. (ν=1)¶	46.6	35.8	14.1	3.7	0.7	0.0004	
		Exp. (ν=2)**	36.7	49.1	12.8	1.3	0.07	0.2	

*For each chromosome, the expected percentages of bivalents with 0, 1, 2, 3 or 4 foci are based on the observed average number of MLH1 foci on that chromosome (Table 1), and the corrected estimate of the interference parameter ν (Table 2) for MLH1 foci on that chromosome. We determined the expected percentages by simulating the positions of MLH1 foci along at least 5000 bivalents for the corrected ν, rounded to an integer value, assuming that MLH1 foci are uniformly distributed along the bivalent (Fig. 1).

†The *P* values in this column represent for each bivalent the probability of finding an as-bad or worse fit of the observed to the expected numbers due to sampling error (χ^2 test; groups were combined if the expected numbers equaled 5 or less).

‡The *P* values in this column represent for each bivalent the probability of finding an as-large or larger difference between the observed values for the wild type and those for *Sycp3*$^{-/-}$ due to sampling error (Fisher's exact test).

§Expected percentages of bivalents with 0, 1, 2, 3 or 4 foci for the corrected estimate of the interference parameter ν.

¶Expected percentages of bivalents with 0, 1, 2, 3 or 4 foci if there were no interference between MLH1 foci (ν=1).

**Lowest integer value of ν for which the expected distribution of the numbers of MLH1 foci per bivalent fits to the observed distribution (i.e. $P>0.05$).

foci are distributed uniformly along the bivalents (which is roughly correct, see Fig. 1I) and that the gamma model applies for the spacing of MLH1 foci, we then estimated for each of the four analyzed chromosomes, in the wild type and *Sycp3*$^{-/-}$, the expected numbers of bivalents with 0, 1, 2, 3 and 4 foci, based on the corrected $\hat{\nu}$ values (corr. ν in Table 2), and the observed average numbers of foci per bivalent (Table 1). For the long chromosomes, we found generally a good fit of the observed with the expected numbers (Table 3). This supports the use of the gamma model and the ν estimates for these chromosomes, and thus confirms the occurrence of strong interference among MLH1 foci on *Sycp3*$^{-/-}$ chromosomes 1 and 2.

For chromosomes 18 and 19, we could not estimate ν from the interfocus distances, because these chromosomes rarely have more than one focus. For these chromosomes we performed a series of simulations based on the observed average numbers of foci per bivalent and increasing integer values of ν. For ν=1 (no interference), the expected frequencies of bivalents with 0 or more than 1 focus were much higher than those observed, both for chromosome 18 and 19, and in both *Sycp3*$^{-/-}$ and wild-type oocytes (Table 3), which indicates positive interference among MLH1 foci on these chromosomes. For wild-type chromosomes 18 and 19, the observed numbers of bivalents with 0, 1, 2, 3 or 4 foci fitted only with the expected numbers for high ν values ($\nu\geqslant16$ for chromosome 18, $\nu\geqslant33$ for chromosome 19). This suggests that in wildtype, interference on chromosomes 18 and 19 is as strong as or stronger than interference on chromosomes 1 and 2. Broman et al. (Broman et al., 2002) inferred similar high ν values for the short chromosomes of wild-type female mice from genetic intercrossover distances. For *Sycp3*$^{-/-}$ chromosome 19, only few MLH1 foci were available for analysis, and the observed distribution of the numbers of foci per bivalent was therefore compatible with a broad range of ν values (Table 3). However, it was not compatible with ν=1 (Table 3), implying that the lower average number of foci per bivalent of *Sycp3*$^{-/-}$ chromosome 19 is not accompanied by total loss of interference. For *Sycp3*$^{-/-}$ chromosome 18, the observed distribution of the numbers of foci per bivalent fitted with the expected distribution for $\nu\geqslant8$, indicating strong interference on this chromosome. Altogether, the observed distributions of the numbers of foci per bivalent are consistent with wild-type interference levels on all four analyzed *Sycp3*$^{-/-}$ chromosomes.

For all analyzed chromosomes, except *Sycp3*$^{-/-}$ chromosome 19, the frequency of bivalents without MLH1 foci was low. Because bivalents without crossovers are generally rare, a mechanism ensuring at least one 'obligate' crossover is sometimes assumed (cf. Jones and Franklin, 2006). However,

for the analyzed wild-type and *Sycp3*$^{-/-}$ chromosomes it is not necessary to assume such a mechanism besides interference itself, because we found in all cases ν values for which the observed numbers of bivalents with 0, 1, 2, 3, and 4 foci fitted with the expected numbers. However, a mechanism ensuring at least one MLH1 focus per bivalent cannot be excluded.

AEs, synapsis and interference among MLH1 foci

Because the reconstruction of bivalents in *Sycp3*$^{-/-}$ oocytes was particularly laborious (see Fig. S1 in supplementary material) (Wang and Höög, 2006), we could analyze only a limited number of bivalents. Nevertheless, the results clearly show that neither full synapsis nor intact axial elements are required for wild-type levels of interference in mouse *Sycp3*$^{-/-}$ oocytes. Furthermore, the SYCP3 protein and the proper localization of SYCP2 are not essential for interference, which fits with a preliminary analysis of the distribution of MLH1 foci among selected SCs with (almost) full synapsis in *Sycp3*$^{-/-}$ oocytes (Wang and Höög, 2006).

The SC and synapsis play a major role in early interference models (Egel, 1995; Fung et al., 2004; Roeder, 1997). However, we found no difference in interference level across synapsed or (partially) unsynapsed stretches, which argues against a role of synapsis in interference, or an effect of a delay in synapsis on the strength of interference (Chua and Roeder, 1997; Conrad et al., 1997). Thus, although we cannot formally exclude the fact that the *Sycp3*$^{-/-}$ cohesin axes were briefly fully synapsed when interference was imposed, our results add to a growing list of diverse observations arguing against a role for synapsis in interference (reviewed by de Boer and Heyting, 2006).

Support for a role of AEs in interference comes from the *Caenorhabditis elegans him-3(me80)* mutant. HIM-3 is thought to be a structural AE protein (Zetka et al., 1999); the *C. elegans him-3(me80)* mutant incorporates reduced amounts of HIM-3 in AEs, and shows reduced levels of crossover interference (Nabeshima et al., 2004). This might suggest that an intact AE structure is essential for wild-type interference levels. However, the mouse *Sycp3*$^{-/-}$ phenotype argues against this: despite grossly abnormal AEs, *Sycp3*$^{-/-}$ oocytes show wild-type levels of interference among MLH1 foci. Also, preliminary evidence in *Tetrahymena* suggests crossover interference in the absence of both SCs and AEs (Loidl and Scherthan, 2004). It is possible that the *C. elegans* HIM-3 protein has roles in interference other than a structural one, or there is a species-specific difference in the role of the intact AE structure in interference.

If neither intact SCs nor intact AEs function in interference, which structure (if any) does? One recent interference model dealing with this question is the stress model (Kleckner et al., 2004), according to which, mechanical stress is generated by expansion of chromatin against some chromatin-constraining structure. Mechanical stress would promote covalent changes in recombination intermediates that lead to crossover formation, and if such a change would occur, it would trigger local stress relief around the involved recombination complex. The stress relief would spread along the bivalent and decrease the probability of the formation of additional crossovers nearby, thus bringing about crossover interference. In this model, the relevant chromatin-constraining structure is essential for generating interference (by withstanding expanding chromatin), and might also be important for conducting the interference signal along the bivalent. The mouse *Sycp3*$^{-/-}$ phenotype shows that the intact AE structure is required neither for generating interference nor for guiding the interference signal. In the context of the stress model this is not surprising, because Kleckner et al. (Kleckner et al., 2004) suggested that expansional stress and stress relief might function in the coordination and spacing of events not only in meiosis, but also in the mitotic cycle, when AEs are not formed. One candidate structure that might be involved in generating and guiding interference is the chromosome scaffold.

Unexpectedly, some MLH1 foci in *Sycp3*$^{-/-}$ oocytes localized to converged cohesin axes without detectable SYCP1 (Fig. 1A-F). This appears to contradict the dependence of MLH1 focus formation on SYCP1 (de Vries et al., 2005). Possibly, SYCP1 colocalized with MLH1 in *Sycp3*$^{-/-}$ oocytes at earlier time points than our measurements, and/or minute amounts of SYCP1 colocalized with MLH1 foci in *Sycp3*$^{-/-}$ mice. That would be consistent with the proposed role of yeast TF protein Zip1 in crossover formation, besides its role in synapsis (Storlazzi et al., 1996).

Materials and Methods

Antibodies and cytological techniques

All antibodies used have been described (de Vries et al., 2005). Oocytes of wild-type and *Sycp3*$^{-/-}$ mice were isolated, spread and incubated for immunofluorescence and FISH as described (de Boer et al., 2006; de Vries et al., 2005). We measured SCs and cohesin axes and processed the images as described (de Boer et al., 2006).

Statistical methods

Estimation of the interference parameter ν and correction of the ν estimates (Table 2) for the limited range of observable interfocus distances have been described (de Boer et al., 2006); the correction results in slightly lower estimates of ν. We determined the distribution of the numbers of foci per bivalent expected for integer values of ν using a macro in Excel (Microsoft), which is available on request from the corresponding author.

We thank N. Vischer (University of Amsterdam) for the Object Image program, F. Lhuissier (Wageningen University) for adapting the program, the animal facilities at Wageningen University for expert technical support, and H. Offenberg and F. Lhuissier for useful comments. The Swedish Research Council financially supported C.H.

References

Ashley, T. and Plug, A. W. (1998). Caught in the act: deducing meiotic function from protein immunolocalization. *Curr. Top. Dev. Biol.* **37**, 201-239.

Baker, S. M., Plug, A. W., Prolla, T. A., Bronner, C. E., Harris, A. C., Yao, X., Christie, D.-M., Monell, C., Arnheim, N., Bradley, A. et al. (1996). Involvement of mouse *Mlh1* in DNA mismatch repair and meiotic crossing over. *Nat. Genet.* **13**, 336-342.

Broman, K. W. and Weber, J. L. (2000). Characterization of human crossover interference. *Am. J. Hum. Genet.* **66**, 1911-1926.

Broman, K. W., Rowe, L. B., Churchill, G. A. and Paigen, K. (2002). Crossover interference in the mouse. *Genetics* **160**, 1123-1131.

Chua, P. R. and Roeder, G. S. (1997). Tam1, a telomere-associated meiotic protein, functions in chromosome synapsis and crossover interference. *Genes Dev.* **11**, 1786-1800.

Conrad, M. N., Dominguez, A. M. and Dresser, M. E. (1997). Ndj1p, a meiotic telomere protein required for normal chromosome synapsis and segregation in yeast. *Science* **276**, 1252-1255.

de Boer, E. and Heyting, C. (2006). The diverse roles of transverse filaments of synaptonemal complexes in meiosis. *Chromosoma* **115**, 220-234.

de Boer, E., Stam, P., Dietrich, A. J. J., Pastink, A. and Heyting, C. (2006). Two levels of interference in mouse meiotic recombination. *Proc. Natl. Acad. Sci. USA* **103**, 9607-9612.

de Vries, F. A. T., de Boer, E., van den Bosch, M., Baarends, W. M., Ooms, M., Yuan, L., Liu, J.-G., Heyting, C. and Pastink, A. (2005). Mouse *Sycp1* functions in synaptonemal complex assembly, meiotic recombination, and XY body formation. *Genes Dev.* **19**, 1376-1389.

Dev, V. G., Tantravahi, R., Miller, D. A. and Miller, O. J. (1977). Nucleolus organizers in *Mus musculus* subspecies and in the RAG mouse cell line. *Genetics* **86**, 389-398.

Egel, R. (1995). The synaptonemal complex and the distribution of meiotic recombination events. *Trends Genet.* **11**, 206-208.

Froenicke, L., Anderson, L. K., Wienberg, J. and Ashley, T. (2002). Male mouse recombination maps for each autosome identified by chromosome painting. *Am. J. Hum. Genet.* **71**, 1353-1368.

Fung, J. C., Rockmill, B., Odell, M. and Roeder, G. S. (2004). Imposition of crossover interference through the nonrandom distribution of synapsis initiation complexes. *Cell* **116**, 795-802.

Higgins, J. D., Sanchez-Moran, E., Armstrong, S. J., Jones, G. H. and Franklin, F. C. (2005). The *Arabidopsis* synaptonemal complex protein ZYP1 is required for chromosome synapsis and normal fidelity of crossing over. *Genes Dev.* **19**, 2488-2500.

Hillers, K. J. (2004). Crossover interference. *Curr. Biol.* **14**, R1036-R1037.

Hunter, N. and Borts, R. H. (1997). Mlh1 is unique among mismatch repair proteins in its ability to promote crossing over during meiosis. *Genes Dev.* **11**, 1573-1582.

Jones, G. H. and Franklin, F. C. (2006). Meiotic crossing-over: obligation and interference. *Cell* **126**, 246-248.

Kleckner, N. and Zickler, D. (2003). Coordinate variation in meiotic pachytene SC length and total crossover/chiasma frequency under conditions of constant DNA length. *Trends Genet.* **19**, 623-628.

Kleckner, N., Zickler, D., Jones, G. H., Dekker, J., Padmore, R., Henle, J. and Hutchinson, J. (2004). A mechanical basis for chromosome function. *Proc. Natl. Acad. Sci. USA* **101**, 12592-12597.

Loidl, J. and Scherthan, H. (2004). Organization and pairing of meiotic chromosomes in the ciliate *Tetrahymena thermophila*. *J. Cell Sci.* **117**, 5791-5801.

McPeek, M. S. and Speed, T. P. (1995). Modeling interference in genetic recombination. *Genetics* **139**, 1031-1044.

Nabeshima, K., Villeneuve, A. M. and Hillers, K. J. (2004). Chromosome-wide regulation of meiotic crossover formation in *Caenorhabditis elegans* requires properly assembled chromosome axes. *Genetics* **168**, 1275-1292.

Page, S. L. and Hawley, R. S. (2004). The genetics and molecular biology of the synaptonemal complex. *Annu. Rev. Cell Dev. Biol.* **20**, 525-558.

Pelttari, J., Hoka, M.-R., Yuan, L., Liu, J.-G., Brundell, E., Moens, P., Santucci-Darmanin, S., Jessberger, R., Barbero, J. L., Heyting, C. et al. (2001). Meiotic chromosomal core consisting of cohesin complex proteins recruits DNA recombination proteins and promotes synapsis in the absence of an axial element in mammalian meiotic cells. *Mol. Cell. Biol.* **22**, 5667-5677.

Roeder, G. S. (1997). Meiotic chromosomes: it takes two to tango. *Genes Dev.* **11**, 2600-2621.

Stam, P. (1979). Interference in genetic crossing over and chromosome mapping. *Genetics* **92**, 573-594.

Storlazzi, A., Xu, L., Schwacha, A. and Kleckner, N. (1996). Synaptonemal complex (SC) component Zip1 plays a role in meiotic recombination independent of SC polymerization along the chromosomes. *Proc. Natl. Acad. Sci. USA* **93**, 9043-9048.

Wang, H. and Höög, C. (2006). Structural damage to meiotic chromosomes impairs DNA recombination and checkpoint control in mammalian oocytes. *J. Cell Biol.* **173**, 485-495.

Yuan, L., Liu, J. G., Zhao, J., Brundell, E., Daneholt, B. and Höög, C. (2000). The murine SCP3 gene is required for synaptonemal complex assembly, chromosome synapsis, and male fertility. *Mol. Cell* **5**, 73-83.

Yuan, L., Liu, J. G., Hoja, M. R., Wilbertz, J., Nordqvist, K. and Höög, C. (2002). Female germ cell aneuploidy and embryo death in mice lacking the meiosis-specific protein SCP3. *Science* **296**, 1115-1118.

Zetka, M. C., Kawasaki, I., Strome, S. and Muller, F. (1999). Synapsis and chiasma formation in *Caenorhabditis elegans* require HIM-3, a meiotic chromosome core component that functions in chromosome segregation. *Genes Dev.* **13**, 2258-2270.